Heterometal Grafted Metalla-ynes and Poly(metalla-ynes)

Subjects: Biochemical Research Methods
Contributor: Rayya Albalushi

Metalla-ynes and poly(metalla-ynes) have emerged as unique molecular scaffolds with fascinating structural features and intriguing photo-luminescence (PL) properties. Their rigid-rod conducting backbone with tunable photo-physical properties has generated immense research interests for the design and development of application-oriented functional materials.

Keywords: metalla-ynes ; poly(metalla-ynes)

1. Main-Chain Systems

Transition metal complexes display a multitude of colorful optical (absorption/emission) and interesting magnetic properties due to the presence of metal ions in different oxidation states [1]. Moreover, multi-dimensional applications of transition metal complexes are well established [2]. It is well demonstrated that when one or more transition metal ions (decorated with suitable auxiliary ligands) are embedded in an organic framework via σ-linkage, new conducting materials are realized with limitless features and properties. Such materials, commonly known as metalla-ynes or poly(metalla-ynes), were studied and reviewed by several groups [3]. Both homo- and heterometallic *σ*-acetylide metal complexes with one or more types of transition metal ions are known in the literature, with a majority on homometallic systems [4][5]. The combination of two transition metals provides an effective way to realize new materials with unique structural features and improved properties such as high solubility and transparency [6]. Although heterometallic poly-ynes containing Ni/Pt and Pd/Pt have been known for a long time [7][8], focus on using other metals has been sparse, possibly due to the challenging synthesis of suitable monomers and/or polymers. In this sub-section, we exemplify the structure and properties of heterometallic molecular systems while clusters [9] are beyond the scope of this paper. Attempts were made to include recent references that have not been covered before [10].

Dixneuf and co-workers [11] reported the first one dimensional Ru(II)/Pd(II) mixed metalla-yne as a yellow oligomer in good yield (84%) and moderate chain length (M_w = 14,800, M_n = 7800). Basic structural characterization showed the formation of mixed metalla-yne but no photo-physical properties were reported. Wong and co-workers [12] reported the very first example of *soluble* rigid-rod heteronuclear Pt(II)/Hg(II) poly(metalla-yne) (**P1**, **Figure 1**) and their corresponding model complexes. The reported white polymer exhibits excellent thermal stability (T_d = 366 ± 5 °C), and polydispersity (M_w = 29,790, M_n = 15,704, **Table 1**). The fluorescence quantum yield of the heterobimetallic polymer (Φ_f = 0.52 in DCM, **Table 1**) was found to be lower than the homometallic *trans* polymers (Φ_f = 2.53 for Hg(II) and 0.62 for Pt(II) in DCM) but higher than the *cis* counterpart (Φ_f = 0.1 in DCM). Similarly, the heterometallic Pt(II)/Hg(II) complex showed a weak triplet emission at room temperature (RT) and a slightly stronger optical power limiting (OPL) performance than the homo-nuclear Hg(II) complexes. The transparency window of the poly-ynes in the visible regime coupled with their OPL performance was achieved by interrupting π- conjugation via copolymerization with Hg and tuning the Pt geometry (*cis* and *trans*).

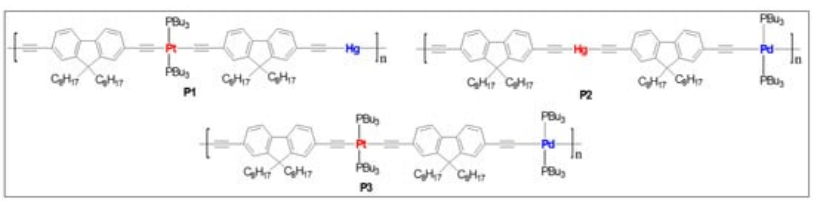

Figure 1. Heterometallic poly(metalla-ynes) **P1**–**P3**.

Table 1. Photoluminescence (PL) data of some selected heterometallic poly(metalla-ynes) **P1–P3** and **P6–P11**.

Code	Metals	Molecular Weight (×10^4)		λ_{abs} (nm)	λ_{ems} (nm)	Lifetime of S_1 (τ^a, ns)	Lifetime of T_1 (τ^b, μs)	Φ (%)	E_g (eV)	Ref.
		M_w	M_n							
P1	**Pt/Hg**	**2.9**	**1.5**	**386**	**409 [a], 542 [b],582 [b]**	**1.23**	**194.38, 202.84**	**0.52**	**3.01**	[12]
P2	**Pd/Hg**	**0.45**	**0.40**	**411**	**430 [a], 544 [b], 578 [b]**	**0.92**	**12.19, 22.71**	**12.60**	**2.85**	[13]
P3	**Pt/Pd**	**2.5**	**1.3**	**415**	**437 [a], 540 [b], 588 [b]**	**0.89**	**193.7, 188.2**	**0.60**	**2.83**	[13]
P6	**Pt/Au**	**-**	**2.4**	**270, 276, 305, 319, 345, 362, 387**	**417 [a], 438[a], 450[a], 539 [a], 548 [b], 587 [b], 625 [b], 642 [b]**	**0.71**	**181.63**	**1.03**	**2.98**	[14]
P7	**Pt/Au**	**-**	**2.7**	**264, 276, 316sh, 377**	**504[a], 504 [b], 545 [b], 563 [b]**	**10370**	**130.80**	**0.62**	**3.00**	[14]
P8	**Pt/Au**	**-**	**2.9**	**253, 262, 276sh, 317, 335**	**405 [a], 425 [a], 455 [a], 495 [a], 534 [a], 456 [b], 492 [b], 507 [b], 527 [b]**	**0.99**	**44.31**	**0.27**	**3.19**	[14]
P9	**Pt/Au**	**-**	**2.1**	**275, 305, 319, 344, 361, 384**	**412 [a], 432 [a], 449sh [a], 542 [a], 584 [a], 548 [b], 586 [b], 619 [b]**	**0.63**	**137.84**	**1.66**	**3.00**	[14]
P10	**Pt/Au**	**-**	**2.4**	**268, 275, 314sh, 373**	**504 [a], 503 [b], 529 [b], 603 [b]**	**6460**	**165.23**	**1.69**	**3.01**	[14]
P11	**Pt/Au**	**-**	**3.1**	**253, 261, 316, 334**	**402 [a], 421 [a], 438 [a], 455 [a], 503 [a], 457 [b], 493 [b], 507 [b]**	**0.72**	**40.14**	**0.30**	**3.12**	[14]

M_w: average weight molecular weight, M_n: number weight molecular weight, λ_{abs}: absorption wavelength peaks, λ_{ems}: emission wavelength peaks, sh: shoulder, a: measured at 298 K, b: measured at 77 K, Φ: quantum yield, E_g: energy gap.

A comparative study on homo- and heterometallic poly-ynes (**P1**–**P3**, **Figure 1**) indicated that Hg(II) and Pt(II) containing poly-ynes are better candidates for OPL than the corresponding Pd(II) poly-ynes as the former display absorption maxima below 400 nm [13]. It was shown that the heterometallic complex **P1** shows better transparency (maximum absorption wavelength (λ_{max}) = 386 nm, **Table 1**) than that of homometallic Pt(II) complexes (**Figure 2**). Theoretical calculations suggested that in heterometallic complexes, the contribution of d_π orbitals to the highest occupied molecular orbital (HOMO) was more from Pd/Pt than the Hg. Conversely, the contribution of p_π orbitals to the lowest unoccupied molecular orbital (LUMO) was more from the Hg fragment, in line with the earlier studies [12].

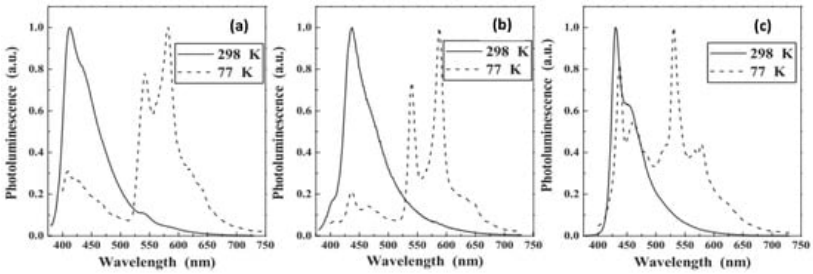

Figure 2. Photoluminescence (PL) spectra at 298 K and 77 K in CH_2Cl_2 for (**a**) **P1**, (**b**) **P3**, and (**c**) **P2**. Reproduced with permission from ref. [13].

In 2005, Vicente et al. [15] reported the very first examples of Pt(II)/Au(I) heterometallic anionic poly(metalla-ynes) **P4** and **P5** (**Figure 3**). The polymers, obtained by reacting Pt(II) *bis*- or *tetra* acetylides with PPN[Au(acac)$_2$] (PPN = *bis*(triphenylphosphine)iminium cation, acac = acetylacetone) were poorly characterized due to the extremely low solubility. The only polymer **P5** (R = Bu) was soluble and could be characterized by nuclear magnetic resonance (^{1}H, ^{13}C, and ^{31}P NMR) and gel permission chromatography (GPC) techniques, which showed comparatively good chain length of the polymers (up to 667 units).

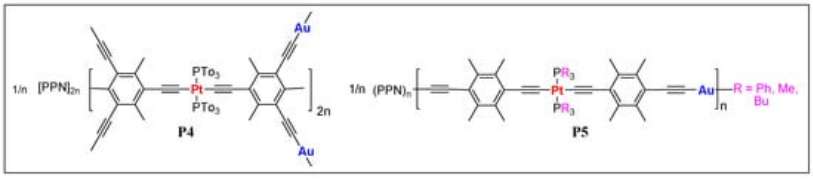

Figure 3. Pt(II)/Au(I) heterometallic anionic poly(metalla-ynes) **P4** and **P5**. (PPN = bis(triphenylphosphine)iminium cation).

Wong and co-workers [14] reported heterometallic Au(I)–Pt(II) poly(metalla-ynes) (**P6**–**P11**, **Figure 4**), in which the impact of merging two different metals can be clearly observed (**Table 1**). Compared to the homometallic systems, Au(I)–Pt(II) poly(metalla-ynes) showed blue-shifted absorption maxima and cut-off absorption wavelengths in solution slightly shifted with respect to monomeric Pt(II) complexes. Merging two different metallic cores also significantly improved the transparency of the resulting material, which was attributed to the weak metal-ligand interactions and conjugation interruption by auxiliary ligands.

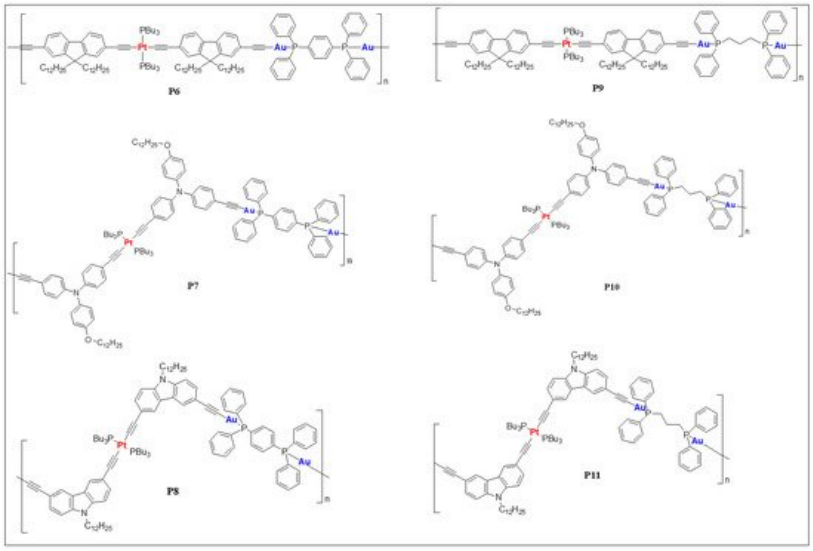

Figure 4. Heterometallic Au(I)–Pt(II) poly(metalla-ynes) (**P6**–**P11**) reported by Wong et al. [14].

2. Side-Chain Systems

2.1. *d-d* Metal-Containing Systems

Compared to the main chain heterometallic systems, dimers and polymers with second organometallic fragments attached via chelating ligand are more common in the literature. Several oligo- and poly(metalla-ynes) bearing heterometallic fragments were synthesized and studied in the past. In this section, we discuss some pertinent examples of both small and large molecular systems with two or more types of metal ions. As observed in the earlier examples, the inclusion of a second metal affects the PL properties. Among *d-d* combinations, the use of Ir(III) and Re(I) with Pt(II) metalla-ynes is very common as the mixed-metal systems show improved photo-physical behavior [16]. It is well established that the photo-physical properties of a material are the function of the molecular structure of the main-chain and pendant ligands. Studies on heterometallic branched complexes indicated that the absorption and emission energies shift to the red upon the incorporation of the Pd(II) fragment moiety [17]. Compared to monometallic Re(I) complexes (maximum absorption wavelength (λ_{absmax}) = 408–418 nm), trimetallic complexes **O1** (R = H or Me, **Figure 5**) exhibit low energy transition at λ_{absmax} = 416–426 nm in solution (**Table 2**). Similarly, in tetrahydrofuran (THF) solution at RT, Re(I) complexes showed maximum emission wavelength (λ_{emmax}) at 625–636 nm (lifetime, τ_0 = < 0.1 µs), while Pd(II)/Re(I) complexes emitted at λ_{emmax} = 628–639 nm (τ_0 = < 0.1 µs, **Table 2**). Heterometallic complex **O2** (**Figure 5**) bearing Pd(II)/Ru(II) core exhibits highly red shifted absorption band (**Table 2**) compared to monometallic Ru(II)-counterpart [18].

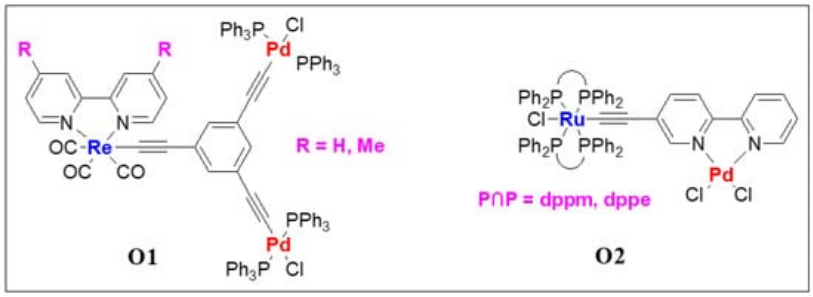

Figure 5. Re(I)/Pd(II) hetero-trimetallic (**O1**) and Ru(II)/Pd(II) heterometallic (**O2**) complexes.

Piazza and coworkers [19] assessed the photo-physical and magnetic properties of Ru(II)/Cu(I) and Ru(II)/Mn(I) couples **O3** and **O4** (**Figure 6**). Interestingly, a long-distance magnetic coupling between the terminal Cu(II) units through Ru(II) fragment was noted. Moreover, heterometallic systems displayed low energy bands in the visible region (**Table 2**). Cu(II) complexes exhibit higher thermal stability compared to Mn(I) complexes.

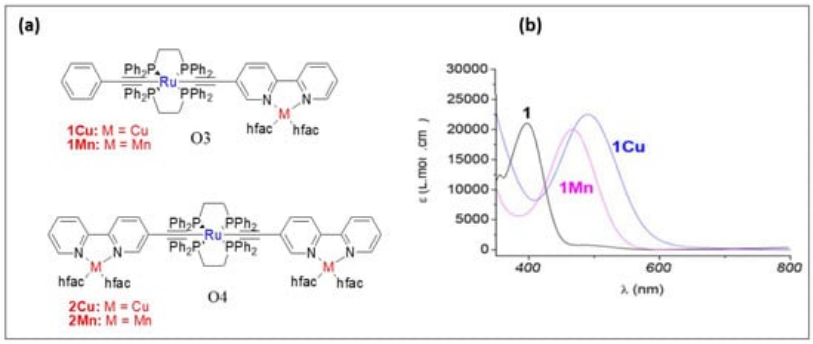

Figure 6. (**a**) Structures of bimetallic and trimetallic Ru/Cu and Ru/Mn complexes **O3** and **O4** and (**b**) the optical absorption spectra (in CH_2Cl_2) of **O3** when M = Cu (1Cu) and Mn (1Mn) along with the corresponding monometallic Ru-bipyridyl compound (**1**). Reprinted (adapted) with permission from Di Piazza, E.; Boilleau, C.; Vacher, A.; Merahi, K.; Norel, L.; Costuas, K.; Roisnel, T.; Choua, S.; Turek, P.; Rigaut, S., Ruthenium carbon-rich group as a redox-switchable metal coupling unit in linear trinuclear complexes. Inorg. Chem. 2017, 56, (23), 14540–14555. Copyright 2017 American Chemical Society.

In contrary to this, theoretical and experimental studies suggest that the two metal centers in binuclear heterometallic Ru(I)/Re(I) complexes **O5**–**O7** (**Figure 7**) are weakly coupled [20]. Chen et al. [21] found that the insertion of one or more heterometal (Re/Ru) reduces the π* energy level in the ethynyl bipyridyl ligand in platinaynes and thus alters the photo-physical properties. For example, complexes (**O8** and **O9**, **Figure 7**) showed a red-shift in optical absorption and longer lifetime (in μs) compared to monometallic platinaynes (**Table 2**). Complex with Pt/Ru couple (λ_{absmax} = 504 nm, λ_{emmax} = 658 nm and τ_0 = < 0.1 μs) showed red shifted absorption and emission compared to Pt/Re λ_{abmax}= 427 nm, λ_{emmax} = 595 nm and τ_0 = < 1.5, 0.22 μs) and Pt (λ_{abmax}= 392 nm, λ_{emmax} = 540 nm and τ_0 = < 0.1 μs) complexes.

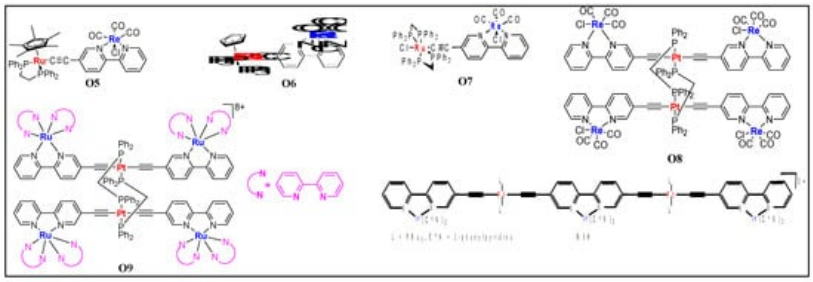

Figure 7. Structures of the *d-d* and *d-f* type heterometallic complexes **O5−O10**.

In addition to these small molecular systems, several polymeric complexes bearing *d-d* metal fragments were also investigated [22]. Complex **O10** (**Figure 8**) is an example of a highly emissive (**Table 2**) pentanuclear complex containing Pt(II) and Ir(III) fragments [23]. An efficient triplet energy transfer between the terminal and central Ir(III) cores through the Pt(II) moiety was reported in such systems.

Table 2. Photoluminescence (PL) data of some selected heterometallic metalla-ynes **O1−O4** and **O8−O10**.

Code	Metals	λ_{abs}(nm)	λ_{ems}(nm)	Lifetime of $S_1(\tau^a$, μs)	Lifetime of $T_1(\tau^b$, μs)	Φ (%)	Ref.
O1 (R = Me)	Pd/Re	236, 284, 336sh, 416	628 [a], 589 [b]	<0.1	0.73	-	[17]
O1 (R = H)	Pd/Re	238, 284, 334sh, 426	639 [a], 594 [b]	<0.1	0.62	-	[17]
O2 (dppm)	Pd/Ru	386	-	-	-	-	[18]
O2 (dppe)	Pd/Ru	389	-	-	-	-	[18]
O3	Ru/Cu	308, 494	-	-	-	-	[19]
O3	Ru/Mn	308, 468	-	-	-	-	[19]
O4	Ru/Cu	308, 494	-	-	-	-	[19]
O4	Ru/Mn	306, 468	-	-	-	-	[19]
O8	Pt/Re	271, 382, 427	595	1.5, 0.22	-	0.0018	[21]
O9	Pt/Ru	243, 291, 360, 504	658	<0.1	-	0.045	[21]
O10	Pt/Ir	255, 315, 415, 435	560 [a], 613 [a], 663 [a],550 [b], 595 [b], 651 [b]	2.3	2.5, 1.9	3.3	[23]

λ_{abs}: absorbtion wavlength peaks, λ_{ems}: emission wavelength peaks, sh: shoulder, a: measured at 298 K, b: measured at 77 K, Φ: quantum yield.

Harvey and coworkers [24] prepared a series of mono- and bimetallic Pt(II)/Ir(III) complexes (**P12**–**P14**, **Figure 8**a) and assessed their photo-physical properties. The photophysical features of the heterometallic complexes were found to be a hybrid of the monometallic complexes used. For instance, Ir(III)-containing 5,5′-bisacetylide complex (Φ = 1.6%, τ = 0.09 μs) showed structureless emission maxima at 638 nm while Pt(II) dimer (Φ = 13.7%, τ = 39.2 μs) showed a blue-shifted structured emission at 561 nm. The introduction of a second luminescent fragment in Pt(II) complex (Φ = 13.7%, τ = 39.2 μs) led to Pt/Ir (Φ = 4%, τ = 1.33 μs) dimer with red-shifted emission at 623 nm. Under similar conditions, polymer **P13**, which is a Bipy containing Pt(II) poly-yne exhibits emission at 561 nm (Φ = 12.8%, τ = 9.2 μs, **Table 3**). Ir-containing polymer **P12** showed emission at 617 nm (Φ = 2.6%, τ = 1.22 μs, **Table 3**) (**Figure 8**b). Later the same group [25] compared the photo-physical and electrochemical properties of complex **P14** (**Figure 8**a). Upon fluorination of the pendant ligand, the nature of the excited state remains the same; however, there were some changes in the absorption and in emission profiles (**Table 3**).

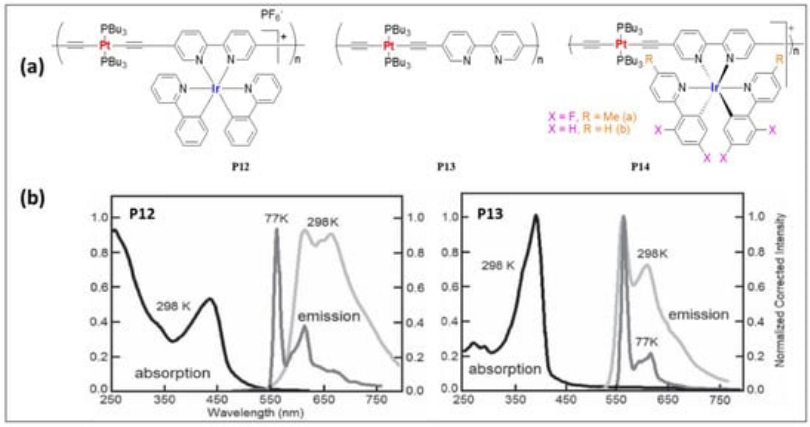

Figure 8. (**a**) Mono- and bi-metallic Pt(II)/Ir(III) polymers (**P12**–**P14**). (**b**) Absorption (298 K) and emission spectra of **P12** and **P13** at 298 and 77 K. Reproduced with permission from ref. [24].

References

1. Zhang, X.; Hou, Y.; Xiao, X.; Chen, X.; Hu, M.; Geng, X.; Wang, Z.; Zhao, J. Recent development of the transition metal complexes showing strong absorption of visible light and long-lived triplet excited state: From molecular structure design to photophysical properties and applications. Coord. Chem. Rev. 2020, 417, 213371.

2. Li, K.; Chen, Y.; Wang, J.; Yang, C. Diverse emission properties of transition metal complexes beyond exclusive single phosphorescence and their wide applications. Coord. Chem. Rev. 2021, 433, 213755.
3. Long, N.J.; Williams, C.K. Metal alkynyl sigma complexes: Synthesis and materials. Angew Chem. 2003, 42, 2586–2617.
4. Haque, A.; Al-Balushi, R.A.; Al-Busaidi, I.J.; Khan, M.S.; Raithby, P.R. Rise of Conjugated poly-ynes and poly(metalla-ynes): From design through synthesis to structure–property relationships and applications. Chem. Rev. 2018, 118, 8474–8597.
5. Haque, A.; Xu, L.; Al-Balushi, R.A.; Al-Suti, M.K.; Ilmi, R.; Guo, Z.; Khan, M.S.; Wong, W.-Y.; Raithby, P.R. Cyclometallated tridentate platinum(II) arylacetylide complexes: Old wine in new bottles. Chem. Soc. Rev. 2019, 48, 5547–5563.
6. Packheiser, R.; Ecorchard, P.; Rüffer, T.; Lang, H. Heteromultimetallic transition metal complexes based on unsymmetrical platinum (II) bis-acetylides. Organometallics 2008, 27, 3534–3546.
7. Sonogashira, K.; Ohga, K.; Takahashi, S.; Hagihara, N. Studies of poly-yne polymers containing transition metals in the main chain. J. Organomet. Chem. 1980, 188, 237–243.
8. Sonogashira, K.; Kataoka, S.; Takahashi, S.; Hagihara, N. Studies of poly-yne polymers containing transition metals in the main chain: III. Synthesis and characterization of a poly-yne polymer containing mixed metals in the main chain. J. Organomet. Chem. 1978, 160, 319–327.
9. Lang, H.; Packheiser, R. Mixed transition metal acetylides connected by carbon-rich bridging units: On the way to heterohexametallic organometallics. Collect. Czech. Chem. Commun. 2007, 72, 435–452.
10. Xu, H.-B.; Deng, J.-G.; Kang, B. Designed synthesis and photophysical properties of multifunctional hybrid lanthanide complexes. RSC Adv. 2013, 3, 11367–11384.
11. Lavastre, O.; Even, M.; Dixneuf, P.H.; Pacreau, A.; Vairon, J.-P. Novel ruthenium-or iron-containing tetraynes as precursors of mixed-metal oligomers. Organometallics 1996, 15, 1530–1531.
12. Zhou, G.J.; Wong, W.Y.; Lin, Z.; Ye, C. White Metallopolyynes for optical limiting/transparency trade-off optimization. Angew. Chem. Int. Ed. 2006, 45, 6189–6193.
13. Zhou, G.J.; Wong, W.Y.; Ye, C.; Lin, Z. Optical power limiters based on colorless di-, oligo-, and polymetallaynes: Highly Transparent materials for eye protection devices. Adv. Funct. Mater. 2007, 17, 963–975.
14. Tian, Z.; Yang, X.; Liu, B.; Zhong, D.; Zhou, G.; Wong, W.-Y. New heterobimetallic Au (I)–Pt (II) polyynes achieving a good trade-off between transparency and optical power limiting performance. J. Mater. Chem. C 2018, 6, 11416–11426.
15. Vicente, J.; Chicote, M.-T.; Alvarez-Falcón, M.M.; Jones, P.G. Platinum (II) and mixed platinum (II)/gold (I) σ-alkynyl complexes. The first anionic σ-alkynyl metal polymers. Organometallics 2005, 24, 2764–2772.
16. Zhou, G.; He, Y.; Yao, B.; Dang, J.; Wong, W.Y.; Xie, Z.; Zhao, X.; Wang, L. Electrophosphorescent Heterobimetallic oligometallaynes and their applications in solution-processed organic light-emitting devices. Chem.–Asian J. 2010, 5, 2405–2414.
17. Chong, S.H.-F.; Lam, S.C.-F.; Yam, V.W.-W.; Zhu, N.; Cheung, K.-K.; Fathallah, S.; Costuas, K.; Halet, J.-F. Luminescent heterometallic branched alkynyl complexes of Rhenium (I)−Palladium (II): Potential building blocks for heterometallic metallodendrimers. Organometallics 2004, 23, 4924–4933.
18. Koutsantonis, G.A.; Jenkins, G.I.; Schauer, P.A.; Szczepaniak, B.; Skelton, B.W.; Tan, C.; White, A.H. Coordinating tectons: Bipyridyl-terminated group 8 alkynyl complexes. Organometallics 2009, 28, 2195–2205.
19. Di Piazza, E.; Boilleau, C.; Vacher, A.; Merahi, K.; Norel, L.; Costuas, K.; Roisnel, T.; Choua, S.; Turek, P.; Rigaut, S. Ruthenium carbon-rich group as a redox-switchable metal coupling unit in linear trinuclear complexes. Inorg. Chem. 2017, 56, 14540–14555.
20. Koutsantonis, G.A.; Low, P.J.; Mackenzie, C.F.; Skelton, B.W.; Yufit, D.S. Coordinating Tectons: Bimetallic Complexes from bipyridyl terminated group 8 alkynyl complexes. Organometallics 2014, 33, 4911–4922.
21. Xu, H.-B.; Zhang, L.-Y.; Chen, Z.-N. Syntheses, characterization and luminescence of Pt–M (M=Re, Ru, Gd) heteronuclear complexes with 5-ethynyl-2,2′-bipyridine. Inorg. Chim. Acta 2007, 360, 163–169.
22. Soliman, A.M.; Fortin, D.; Harvey, P.D.; Zysman-Colman, E. Hybrid charged heterometallic Pt–Ir complexes: Tailoring excited states by taking the best of both worlds. Chem. Commun. 2012, 48, 1120–1122.
23. Soliman, A.M.; Fortin, D.; Zysman-Colman, E.; Harvey, P.D. Unexpected evolution of optical properties in Ir–Pt complexes upon repeat unit increase: Towards an understanding of the photophysical behaviour of organometallic polymers. Chem. Commun. 2012, 48, 6271–6273.

24. Soliman, A.M.; Fortin, D.; Zysman-Colman, E.; Harvey, P.D. Photonics of a conjugated organometallic Pt–Ir polymer and its model compounds exhibiting hybrid CT excited states. Macromol. Rapid Commun. 2012, 33, 522–527.
25. Soliman, A.M.; Zysman-Colman, E.; Harvey, P.D. Strategic modulation of the photonic properties of conjugated organometallic Pt–Ir polymers exhibiting hybrid ct-excited states. Macromol. Rapid Commun. 2015, 36, 627–632.

Retrieved from https://encyclopedia.pub/entry/history/show/37384